Thermoelectric exhaust-gas energy recovery: An integrated approach

Thermoelectric exhaust-gas energy recovery: An integrated approach

A. V. Powell, A. Kaltzoglou, P. Vaqueiro, G. Min, J. Garcia-Cañadas, R. K. Stobart, J. Li, G. Dong, and A. Wijewardane

Citation: AIP Conference Proceedings **1449**, 505 (2012);

View online: https://doi.org/10.1063/1.4731604

View Table of Contents: http://aip.scitation.org/toc/apc/1449/1

Published by the American Institute of Physics

Thermoelectric Exhaust-Gas Energy Recovery: An Integrated Approach

A.V. Powell[a], A. Kaltzoglou[a], P. Vaqueiro[a], G. Min[b], J. Garcia-Cañadas[b], R.K. Stobart[c], J. Li[c], G. Dong[c] and A. Wijewardane[c]

[a]*Department of Chemistry & Centre for Advanced Energy Storage and Recovery, Heriot-Watt University, Edinburgh EH14 4AS, UK*
[b]*School of Engineering, Cardiff University, Cardiff CF24 3AA, UK*
[c]*Department of Aeronautical &Automotive Engineering, Loughborough University, Loughborough LE11 3TU, UK*

Abstract. Here we describe the first results from an interdisciplinary project that seeks to develop a skutterudite-based thermoelectric (TE) energy recovery system for a vehicle exhaust stream. Filled skutterudites have been prepared and characterised and their thermal stability evaluated. Thermoelements fabricated from these skutterudites have been used to evaluate the compatibility of materials required for the construction of TE modules. The results of modelling studies for the optimization of heat exchanger design and the creation of a component in the loop test facility are also described.

Keywords: Thermoelectric, Skutterudites, Energy Recovery, Exhaust System.
PACS: 84.60.Rb, 88.05.Bc, 81.70.-q

INTRODUCTION

Thermoelectric (TE) devices are attractive candidates for a system to recover waste heat from the exhaust stream of a combustion engine. However, a major limitation on the implementation of TE energy recovery is the TE performance of materials from which devices may be constructed. The majority of commercial devices are based on Bi_2Te_3 whose performance peaks at relatively modest temperatures ($ZT_{max} \approx 0.9$ at 293 K) and shows significant degradation at exhaust stream temperatures. Recently, skutterudites have emerged as attractive candidates for high-temperature energy recovery systems [1]. The skutterudite structure (Figure 1(a)) of vertex-linked, cation centred octahedra of overall stoichiometry MX_3 contains large voids. These can accommodate a variety of filler species yielding compounds, $G_xM_4X_{12}$, that significantly reduce the thermal conductivity without impairing the transport properties, thereby favouring technologically-viable values of *ZT*.

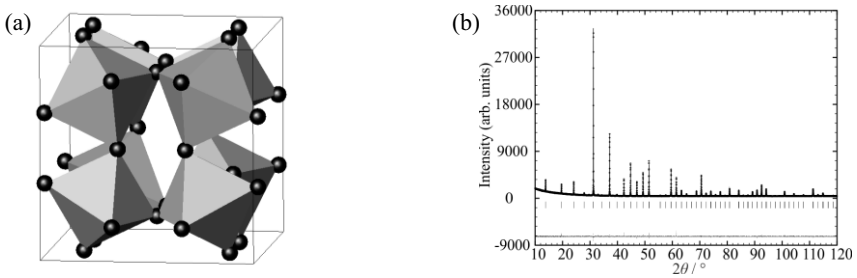

FIGURE 1. (a) Polyhedral Representation of the Skutterudite Structure and (b) Rietveld Analysis of Powder X-ray Diffraction Data for the Filled Skutterudite $Yb_{0.19}Co_4Sb_{12}$ (Space Group $Im\bar{3}$, a = 9.04572(3) Å, χ^2 = 1.68).

The development of a practical thermoelectric generator (TEG), even when high-performance materials are available, poses significant technical challenges. In particular, suitable construction materials and fabrication techniques need to be identified for novel TEs such as filled skutterudites to be integrated into a device, whilst the elevated temperature at which such devices are required to operate also imposes considerable demands, particularly with regard to stability to oxidation and sublimation. Implementation of a TE energy recovery system also requires careful consideration of the heat-exchanger design to maximize energy transfer, whilst the impact of the device on engine performance needs to be evaluated and optimized in order to ensure a net gain in efficiency. Here we present

9th European Conference on Thermoelectrics
AIP Conf. Proc. 1449, 505-508 (2012); doi: 10.1063/1.4731604

the first results from an inter-disciplinary project that brings together materials chemists, TE specialists and automotive engineers that seeks to address these challenges.

RESULTS

Our initial investigations have focused on the skutterudites $Yb_{0.19}Co_4Sb_{12}$ and $Ce_{0.8}Fe_3CoSb_{12}$, which represent the state-of-the-art *n*- and *p*-type materials respectively. Focusing on materials with proven performance has allowed us to progress with the identification and evaluation of potential materials for module construction and in the development of methodologies for fabrication. Oxidation was initially observed during synthesis, yielding materials with up to 3% by weight of binary oxides. However, careful control of the synthetic conditions has allowed us to produce essentially oxide-free phases.

Materials Synthesis and Characterisation

Co_4Sb_{12}, $Yb_{0.19}Co_4Sb_{12}$ and $Ce_{0.8}Fe_3CoSb_{12}$ were synthesized by mixing the appropriate elements in glassy carbon crucibles which were then sealed into evacuated silica tubes (< 10^{-4} Torr). Preparation of Co_4Sb_{12} and $Yb_{0.19}Co_4Sb_{12}$ was effected at 1073 K for 1 day, followed by annealing at 873 K for 3 days. $Ce_{0.8}Fe_3CoSb_{12}$ was prepared by heating at 1273 K for 12 hours, followed by quenching in water and annealing at 873 K for 4 days. All products were characterised by powder X-ray diffraction (Bruker D8 Advance, Cu-$K_{\alpha 1}$ radiation), which in conjunction with Rietveld analysis, confirmed the products to be phase-pure skutterudites (Figure 1(b)). Samples for physical property measurements were loaded into graphite dies and hot-pressed at 900 K (60 MPa, 30 min) under a N_2 atmosphere. The densities of the pellets reach *ca.* 95% of crystallographic values. Electrical resistivity and Seebeck coefficient measurements were performed over the temperature range 100 – 360 K (Figure 2(a) and 2(b)) and thermal conductivity measurements (Anter Flashline 3000) were performed over the temperature range 373 – 750 K. The electrical resistivity measurements are consistent with metallic behaviour for $Yb_{0.19}Co_4Sb_{12}$ and $Ce_{0.8}Fe_3CoSb_{12}$, with values an order of magnitude lower than for Co_4Sb_{12}. The filler atoms (Yb and Ce) also reduce the thermal conductivity significantly from that of Co_4Sb_{12}. The power factors (S^2/ρ) and *ZT* values for the three compounds are presented in Table 1. The value of *ZT* for $Yb_{0.19}Co_4Sb_{12}$ at 350 K is close to that reported by Nolas *et al.* [2] (*ZT* = 0.29 at 350 K) whereas that for $Ce_{0.8}Fe_3CoSb_{12}$ is slightly lower than the highest reported value [3]. The *ZT* values at 350 K indicate that these materials should exhibit high-temperature performance comparable with literature reports ($ZT_{max} \approx 1$ at 600 K and 700 K for $Yb_{0.19}Co_4Sb_{12}$ and $Ce_{0.8}Fe_3CoSb_{12}$ respectively).

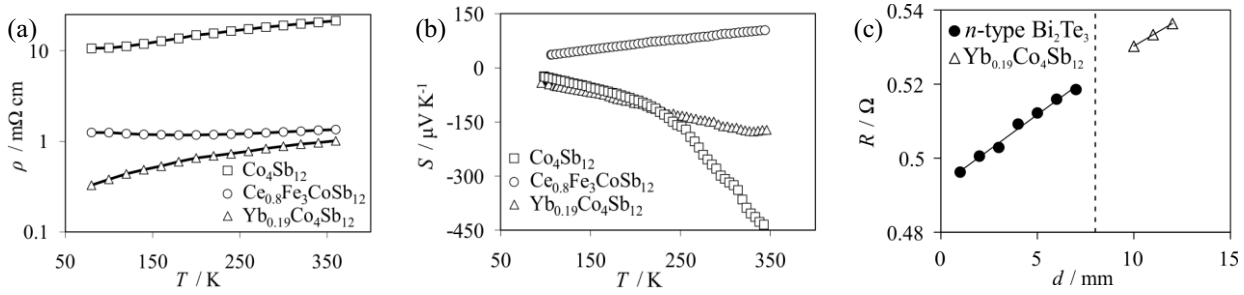

FIGURE 2. Electrical Measurements for Skutterudite Samples: (a) Resistivity, (b) Seebeck Coefficient and (c) the Resistance across a Linear Junction of Bi_2Te_3 and Skutterudite Thermoelements, Illustrating the Discontinuity at the Contact Point (8 mm).

TABLE 1. Thermoelectric Parameters for Skutterudite Samples at 350 K.

Compound	$S^2\rho^{-1}$ / mW m^{-1} K^{-2}	κ^a / W m^{-1} K^{-1}	*ZT*
$Yb_{0.19}Co_4Sb_{12}$	3.06	3.1	0.35
$Ce_{0.8}Fe_3CoSb_{12}$	0.82	2.3	0.12
Co_4Sb_{12}	0.88	9.0	0.03

[a] Values of κ at 350 K were obtained by extrapolation from measured values at 373 K

High-temperature decomposition studies were performed on a DuPont 951 thermogravimetric analyser (TGA). The samples were loaded into silica crucibles and heated in a rate of 2 K min^{-1} up to 1200 K under O_2 flow (60 mL min^{-1}). The onset of oxidation, as evidenced by the sample beginning to gain weight, occurs at *ca.* 500 K, 650 K, and 650 K for $Ce_{0.8}Fe_3CoSb_{12}$, $Yb_{0.19}Co_4Sb_{12}$ and Co_4Sb_{12} respectively. The residues from the TGA were identified

as mixtures of SbO_2, Sb_2O_5, $CoSb_2O_6$ (and $FeSb_2O_6$ for $Ce_{0.8}Fe_3CoSb_{12}$) by powder X-ray diffraction. These investigations suggest a relatively low upper limit to the operating temperature of a skutterudite-based device in air.

Module Fabrication

The selection of suitable materials for solders, barrier layers and electrodes, is critical in ensuring that the intrinsic materials' performance is reflected in the performance of the module, whilst the development of appropriate soldering methodologies is required to avoid degradation of the material through oxidation or sublimation. Initially, two commercial solders have been investigated: $Pb_{93.5}Sn_5Ag_{1.5}$ alloy (T_m = 573 K, Multicore) and $Ag_{59}Cu_{27.25}In_{12.5}Ti_{1.25}$ Incusial ABA (T_m = 973 K, Wesgo Metals). Following polishing and cleaning of $Yb_{0.19}Co_4Sb_{12}$ (*n*-type) and $Ce_{0.8}Fe_3CoSb_{12}$ (*p*-type) thermoelements with *i*-propanol and acetone, a barrier layer of silver (*ca*. 5 μm) was deposited by electroplating. A resin-based flux was then spread on the surface and a piece of solder sandwiched between the thermoelement and a copper foil which serves as the electrode. This arrangement was clamped and introduced into an evacuated quartz tube furnace. For the $Pb_{93.5}Sn_5Ag_{1.5}$ solder, the assembly was heated to 713 K for 10 minutes, whilst for $Ag_{59}Cu_{27.25}In_{12.5}Ti_{1.25}$, a temperature of 1093 K was used. After cooling, significant degradation of the thermoelements was evident in the assembly heated to 1093 K, the origin of which may lie in oxidation and sublimation processes or in side reactions of the skutterudites with the copper electrodes or solder. Performing the soldering under high vacuum (10^{-5} Torr) or under an argon atmosphere did not prevent degradation nor did plating the entire skutterudite thermoelement with nickel. The contacts obtained with the lower melting point solder show excellent mechanical strength. The contact resistance was evaluated using a four-probe DC method. A skutterudite thermoelement was soldered to one of *n*-type Bi_2Te_3 in a linear array, using nickel as the barrier layer for Bi_2Te_3. Measuring the resistance as a function of distance along the linked array (Figure 2(c)) shows the expected linear behaviour along the length of each of the two thermoelements, with a discontinuity at the contact point due to the contact resistance, the magnitude of which is estimated at 8×10^{-5} Ω cm^2.

Modelling Studies

Cooling of the main exhaust gas flow can interfere with the exhaust gas catalytic processes, requiring careful control measures to be adopted in order to utilize the excess energy which is available. However, in a modern engine, exhaust gas is recirculated to the engine inlet (exhaust gas recirculation (EGR)) to reduce NO_x emissions. As the re-circulated gas requires cooling, it is an ideal candidate for energy recovery [4]. EGR coolers have been designed to be compact and highly efficient: they are therefore an excellent starting point for design of efficient heat transfer to a TEG. Given the multi-parameter nature of the problem, the advantages of a TE device can only be fully explored if it is placed in the context of its operation in a working engine. The engine environment is particularly demanding and initial ex-situ evaluation is desirable to predict performance prior to deployment of robust hardware. Therefore we are adopting a component in the loop (CIL) methodology in which a simulated model of the device is linked to the engine and data from bench tests of materials and modules used for real-time modelling on a computer connected to the engine control system. The device outputs are calculated and fed back into the experimental hardware as if the device were in situ.

Heat Exchanger Design

Heat transfer plays a key role in optimising the energy recovery from an exhaust stream. Initial investigations of a TEG using a corrugated open-pipe architecture indicated that the power output was too low to be useful [5]. Therefore, an alternative plate-fin design (Figure 3(a)) was modelled (Star-CCM+ 6.02.009 software) and analysed for different hot and cold side temperatures (Table 2), using parameters for commercially available Bi_2Te_3 TE modules (Hi-Z). This architecture yields higher power outputs than obtainable with the corrugated pipe design.

Operating Conditions for a TEG

The non-road transient cycle (NRTC) represents the typical operating conditions of a non-road diesel engine and provides an indication of the temperature and availability of the EGR gas flow under the varying conditions of load and speed. For a Caterpillar C6.6 engine, data predict the hot-side temperature of the TE module varies between 393 K and 923 K, with a corresponding variation in the energy available. In order to evaluate the impact on engine performance of a TEG and investigate how the power output is affected by engine operating parameters, we have

created a CIL test facility, shown schematically in Figure 3(b). This will serve as a rapid prototyping facility for optimization of a TEG system, thereby reducing development time. A real-time TEG model was constructed using xPC technology and can be used to predict power output, outlet temperature and pressure of a given TEG. This allows the temperature, pressure and mass flow of the EGR path to be controlled to simulate the aftermath of the proposed TEG system, without the need to install TEG hardware, thereby enabling the impact on engine performance to be evaluated. A real-time neural network model of the TEG has been created in order to adjust the EGR cooler to perform as a TE device. This allows engine performance with an operational TEG to be evaluated and optimised by changing the TE material properties in the virtual TEG under practical engine conditions. Once performance data for new skutterudite-based TE modules become available, these will be incorporated into our modelling studies.

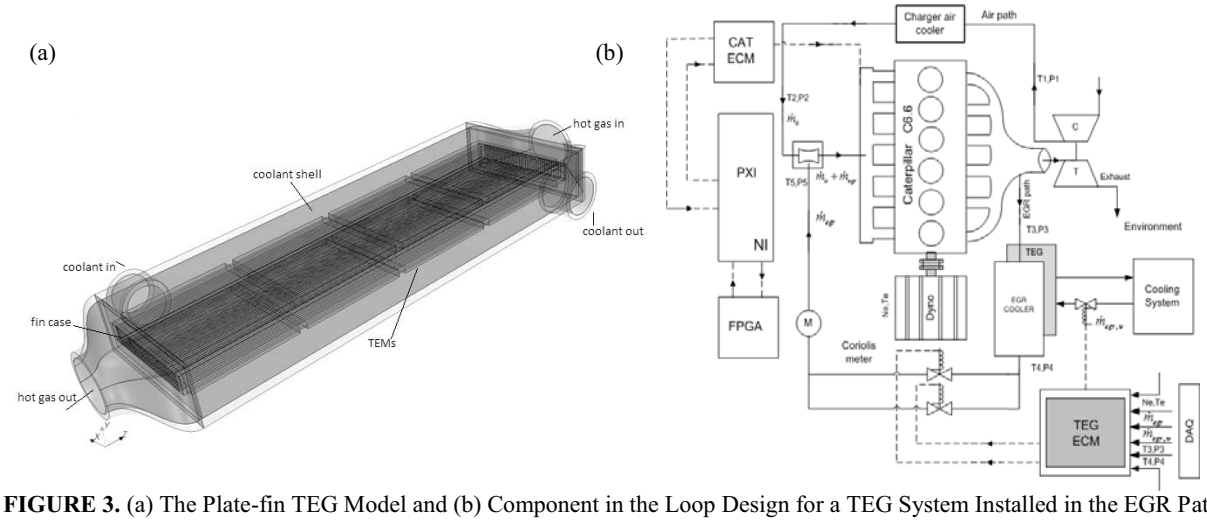

FIGURE 3. (a) The Plate-fin TEG Model and (b) Component in the Loop Design for a TEG System Installed in the EGR Path.

TABLE 2. Calculated Power Output for Different Conditions of Exhaust Gas and Coolant Temperatures (*T*), Mass Flow Rates (*M*) and Thermoelectric Figure-of-Merit (*ZT*).

	Hot gas		Coolant			
Case	***M* / Kg s^{-1}**	***T*/K**	***M* / Kg s^{-1}**	***T*/K**	***ZT***	**Power/W**
1	0.05	700	0.2	300	0.97	139
2	0.05	700	0.5	300	0.97	151
3	0.05	700	0.7	300	0.97	165
4	0.05	700	0.2	300	0.97	150
5	0.05	700	0.2	300	0.97	104
6	0.05	700	0.2	300	0.97	139
7	0.05	700	0.2	300	0.97	139
8	0.01	700	0.2	300	0.97	36
9	0.05	600	0.2	300	0.97	83
10	0.05	500	0.2	300	0.97	41
11	0.05	700	0.2	300	1.87	277
12	0.05	700	0.2	300	2.83	415

ACKNOWLEDGMENTS

We thank the UK Engineering and Physical Sciences Research Council for financial support (EP/H050396).

REFERENCES

1. J.R. Sootsman, DY Chung and M.G. Kanatzidis, *Angew. Chem.* **48**, 8616-8639 (2009).
2. G.S. Nolas, M. Kaeser, R.T. Littleton and T.M. Tritt, *Appl. Phys. Lett.* **77**, 1855-1857 (2000).
3. B.C. Sales, D. Mandrus, B.C. Chakoumakos, V. Keppens and J.R. Thompson, *Phys. Rev B* **56**, 15081-15089 (1997).
4. Q.E. Hussain, D.R. Brigham and C.W. Maranville, *SAE Special Publication SP-2235*, Paper 2009-01-1327 (2009).
5 . R.K. Stobart, A. Wijewardane and C. Allen, *SAE Special Publication SP-2275*, Paper 2010-01-0833 (2010).